Active mirrors for on-orbit alignment of the second generation Wide Field and Planetary Camera

James L. Fanson and John 1. Trauger X.49594

Jet Propulsion Laboratory, California Institute of Technology
4800 Oak Grove Drive, Pasadena, California 91109

ABSTRACT

Correcting the spherical aberration of the Hubble Space Telescope (HST) requires precise optical alignment and stability. To assure that the required alignment can be achieved and maintained on-orbit, the pickoff mirror and three of the four fold mirrors of the second generation Wide Field and Planetary Camera (WI? PC-2) have been made actively controllable in tip and tilt. The Pickoff Mirror Mechanism (PO MM) and the Articulating Fold Mirrors (AFMs) are commanded from the ground to their required positions once the WFPC-2 is installed in the HST. The POMM is a set-and-forget device that utilizes stepper motors, while the AFMs are maintained in position by the continuous application of control voltages to electrostrictive ceramic actuators. This paper describes the assembly level testing and calibration of the AFMs, and the development of a software tool that generates the commands for adjusting the positions of the POMM and AFMs to achieve system level optical alignment. Our experience with the POMM and AFMs through system level calibration and testing of the WFPC-2 instrument is de-scribed.

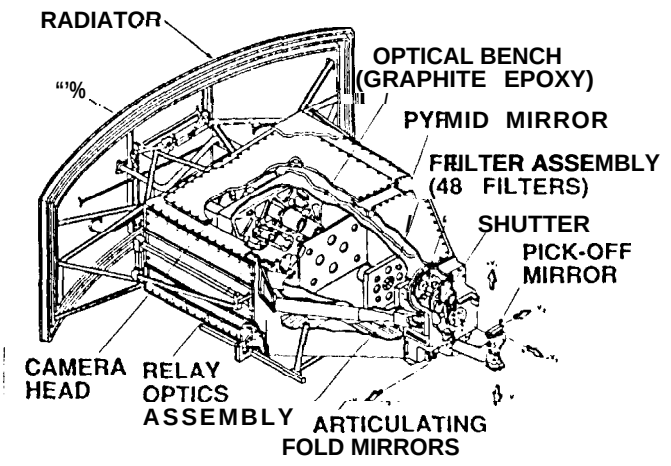

Fig. 1. Cutaway view of WFPC-2 instrument.

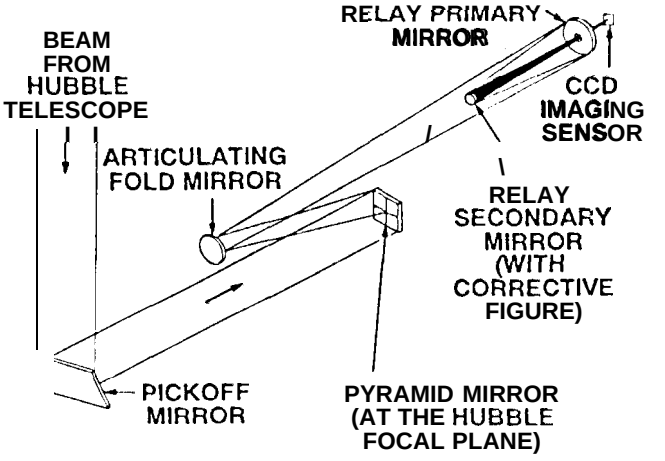

Fig. 2. Typical optical train of WFPC-2.

1. INTRODUCTION

The Wide Field and Planetary Camera (WF/PC) is one of five scientific instruments in the Hubble Space Telescope (11ST), providing a large (152x 152 arc second) field of view at the center of the HST focal plane. By the time HST was launched in 1990, the WFPC-2 (similar to WF/PC but with a number of science enhancements[1]) was being built at the Jet Propulsion Laboratory. The significance of WFPC-2 changed dramatically when it was discovered that the HST primary mirror suffered from 1/2 wave RMS of spherical aberration, seriously impairing the optical performance of the telescope and its instruments.[2] It was quickly realized that by making a minor change to the WFPC-2 optical design, it would theoretically be possible to correct the HST wavefront error and restore the imaging performance to nearly the original specifications. Moreover, since the WFPC-2 was already well along in fabrication, an opportunity existed for a relatively quick and low cost fix to the HST's imaging problem by replacing WF/PC with WFPC-2 during a routine servicing mission, scheduled for 1993. Fig, 1 shows a cutaway view of the WFPC-2 instrument.

The method for correcting the HST wavefront error has been detailed elsewhere;[3,4] it is useful to visualize the approach as that of cancelling one error (in the HST) with an opposite "error" placed on onc of the WFPC-2 mirrors. This is straightforward in principle, but is made difficult in practice by the large magnitude of the error that

Fig. 3. Pickoff Mirror Mechanism (POMM).

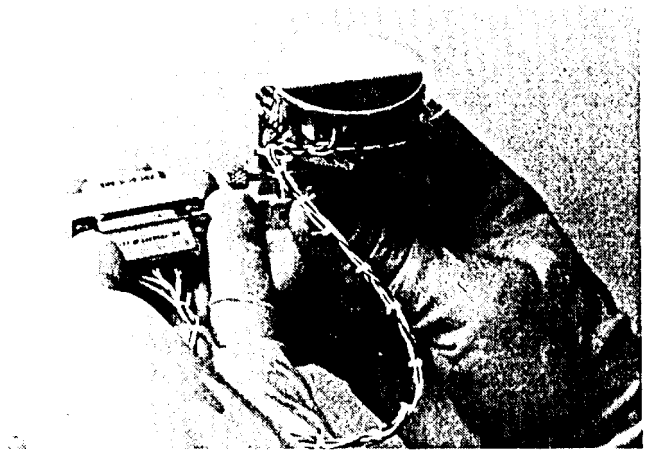

Fig. 4. Articulating Fold Mirror (AFM).

must be corrected. It was determined by calculation that the alignment precision required to effect the wavefront correction was an order of magnitude more stringent than the original tolerances for WFPC-2, and represented a degree of alignment stability well beyond what the WFPC-2 had been designed to deliver. In addition, circumstantial evidence suggested that the on-orbit alignment of WF/PC was drifting over time; similar drifts in WFPC-2 could render the correction ineffective. A means of guaranteeing on-orbit alignment was needed.

Four active mirrors--the Pickoff Mirror Mechanism (POMM) and three Articulating Fold Mirrors (AFMs)--together assure that WFPC-2 can be aligned within the required tolerance to restore the I-1ST imaging performance across the entire 152 arc second field of view. 'I'he detailed design of the AFM has been reported previously.[5] The remainder of this paper describes the active alignment approach, the functional requirements for the POMM and the AFM, the calibration of the AFM as an assembly, the development of an analytical tool for generating commands to align the WFPC-2 optical trains, and experience with the POMM and AFMs through system level environmental and calibration testing of the WFPC-2 instrument.

2. FIXING HUBBLE-- ALIGNMENT 1S CRITICAL

The WFPC-2 instrument consists of three f/12.9 (wide field) and one f/28.3 (planetary) optical trains that must be in alignment simultaneously. A typical optical train is depicted in Fig. 2. The optical design images the pupil of the HST onto the secondary mirror of the relay optics. Each secondary mirror is polished to a shape that exactly matches the error in the HST primary mirror. If the exit pupil is centered on the secondary mirror, then the image formed at the focal plane is well corrected. If the pupil is offset to onc side (pupil shear), then the image formed at the focal plane exhibits coma. The effect of pupil shear on the point spread function (PSF) is shown in Fig. 5. In order to restore the Hubble imaging performance to its original specifications, the on-orbit pupil shear resulting from all sources cannot exceed 0.44 percent of the pupil diameter;[6] this is equivalent to 51 microns of lateral motion at the f/28.3 secondary mirror. The coma that develops in the PSF can be clearly seen from the first Airy ring of Fig. 5b. For comparison, the spherically aberrated PSF corresponding to the as-built HST is shown in Fig. 5d.

The location of the HST optical axis is not known to sufficient accuracy to ensure that the 11ST exit pupil will be adequately aligned with the optical axis of the WFPC-2 instrument. This so called "latch error" is remedied by giving the pickoff mirror a two-axis tilt capability via the Pickoff Mirror Mechanism (POMM) shown in Fig. 3. The POMM can effectively steer the HST pupil into alignment with WFPC-2. Since each of the four optical trains shares the same pickoff mirror, the POMM translates all four pupil images in the same direction by equal amounts with respect to the four relay optics secondary mirrors. In principle, if all four optical trains were perfectly aligned with respect to each other on the ground, and remained in alignment through launch and transition to orbital conditions, then adjustment of the POMM would be sufficient to align WFPC-2. In practice, however, perfect alignment was not achieved, and passive stability through launch and transition to orbital conditions cannot be guaranteed.

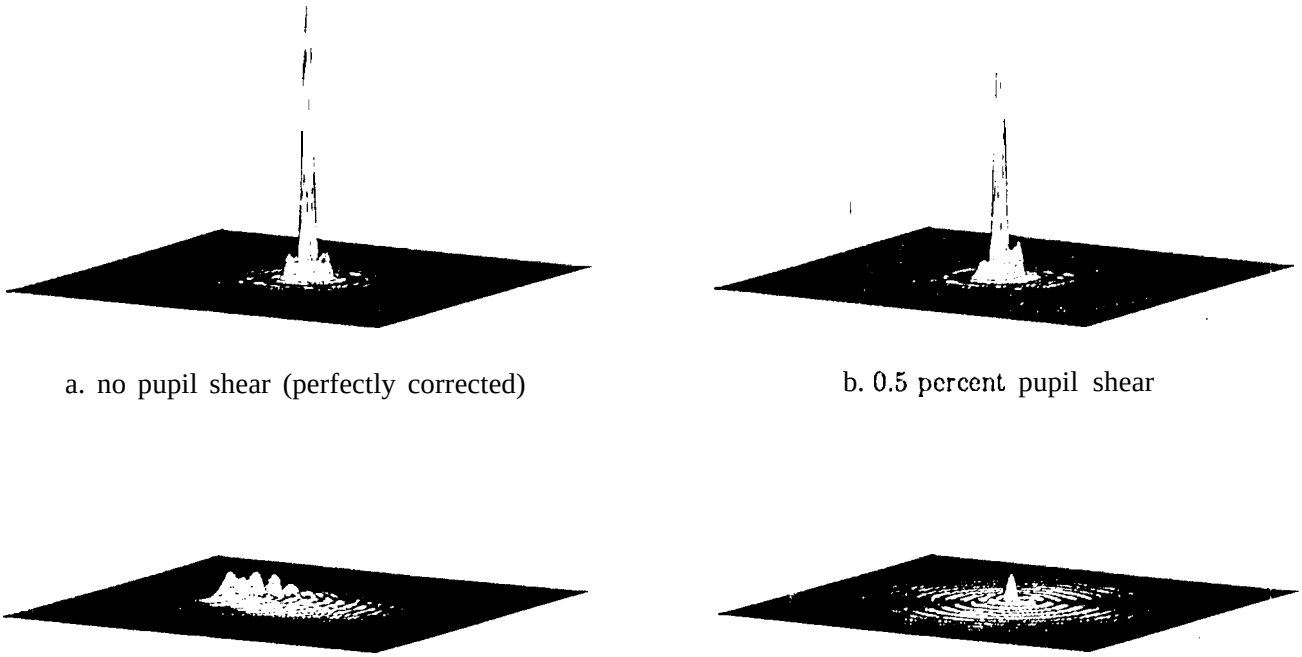

a. no pupil shear (perfectly corrected)

b. 0.5 percent pupil shear

c. 5.0 percent pupil shear

d. spherically aberrated HST without correction

Fig. 5. Various point spread functions computed for the f/28.3 optical train. Grid spacing corresponds to 5 μm at the focal plane (1/3 pixel size).

2.1 Active alignment approach

Alignment of the four optical trains is accomplished in two stages. First, the POMM is adjusted to align one of the four channels; then the Articulating Fold Mirrors (AFMs) are adjusted to bring the remaining three channels into alignment. The Articulating Fold Mirror, shown in Fig. 4, replaces the fixed fold mirror in the optical train and permits the pupil in that channel to be independently positioned. The AFMs correct "differential" pupil shear, and provide a degree of redundancy should the POMM fail. The optical train aligned via the POMM dots not require an AFM, and since packaging constraints precluded an AFM in wide field camera channel #2 (WFC2), this channel was selected for POMM alignment. AFMs arc located in wide field camera channels #3 and #4 (WFC3 and WFC4), and planetary camera channel #1 (PC 1).

Pupil misalignment produces corns in the image as illustrated in Fig. 5. Analysis of star images taken by the four WFPC-2 CCDs therefore provides a direct means of determining the amount and direction of pupil shear in each channel. Once the pupil shear is known, it is a straightforward matter to determine the required mirror adjustments. If the active alignment remains sufficiently stable, no further adjustment of the mirrors is required.

3. ACTIVE MIRROR FUNCTIONAL. REQUIREMENTS

3.1 Top level functional requirements

Since the "latch error" represents a larger source of misalignment than the differential pupil shear from channel to channel, the POMM is required to have a greater range of motion than the AFM. But, because the POMM causes all four pupil images to move in common mode fashion, correcting the pupil shear in WFC2 causes the relative pupil shear in that channel to be transferred (vectorially added) to the pupil shear in the remaining three channels— potentially doubling the magnitude of the pupil shear that must be corrected by the AFMs.

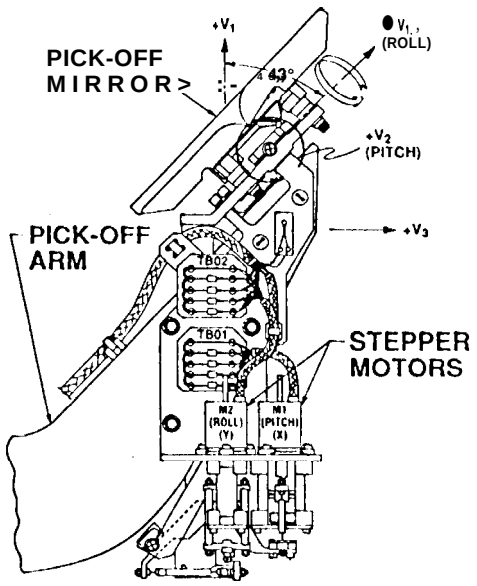

Fig. 6. Schematic of POMM.

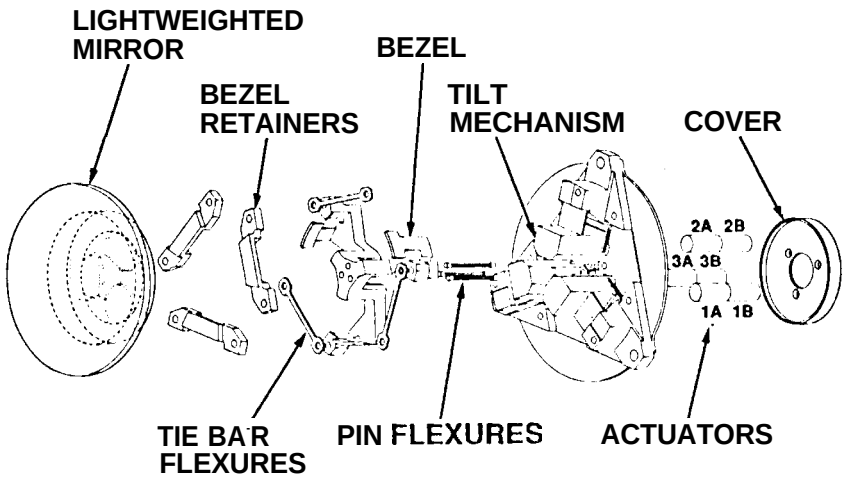

Fig. 7. Exploded view of Articulating Fold Mirror.

The top level functional requirements and operating characteristics for the POMM and the AFM arc given in Table 1. In several instances, the as-built performance is substantially better than the specification. For example, the tilt range of the AFM is temperature dependent (see section 3.3), and at the cold end of the operating temperature range, the tilt range exceeds ±250 arc sec (±5.8 percent pupil shear). Notice that there is no ground-to-orbit stability requirement for the POMM, whereas wc have attempted to minimize differential pupil shear by requiring such stability of the AFM. Notice also that' the AFMs are required to return to their 'home' position in the event of a failure in their control electronics.

"Operational alignment stability for the active mirrors is broken into short term stability (3000 see), and long term stability. Short term stability is driven by the requirement that the image remain stable on the detector to ±0.1 pixel during an exposure; long term stability is based on maintaining pupil shear correction.

Table 1. Functional rcquircrrlcnts/characteristics for POMM and AFM

	POMM	AFM
Requirements:	tip/tilt range ±900 arc sec (±4.4 mrad)	±206 arc sec (±1 mrad)
	short, term (3000 sec) stability +0.18 arc see"	±0.86 arc sec
	long term stability ±6 arc sec	±13.6 arc sec
	ground-to-orbit stability n/a	±10 arc sec
	repeatability ±1 arc sec	±2 arc sec
	failsafe n/a	return to home position
Characteristics:	tilt step size 12 arc scc	<2 arc sec (variable)
	range of correctable pupil shear ±21%	±4.8%
	pupil shear/step 0.27%	n/a
	pupil shear/arc sec 0.023'%	0.023%
	arc see/pixel* 2.1	7.5

• values correspond to f/28.3 channel

3.2 Pickoff Mirror Mechanism design

The Pickoff Mirror Mechanism (POMM) provides tip and tilt control of the pickoff mirror. The mechanism is located at the end of the pickoff arm as shown in Fig. 6. Stray light requirements restrict the POMM to lie entirely

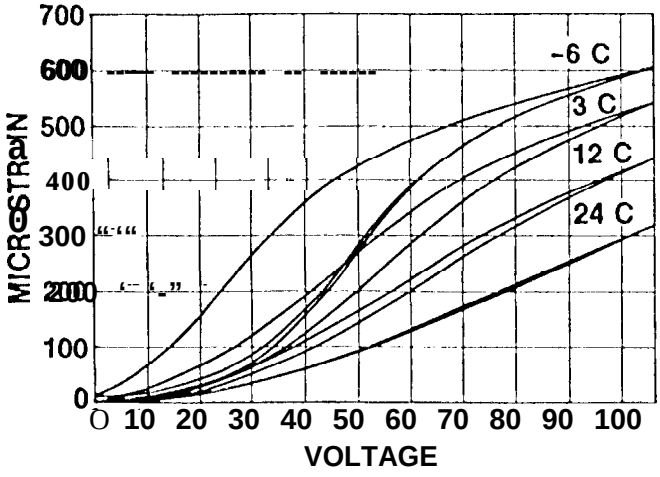

Fig. 8. Electrostrictive actuator strain vs. voltage at various temperatures.

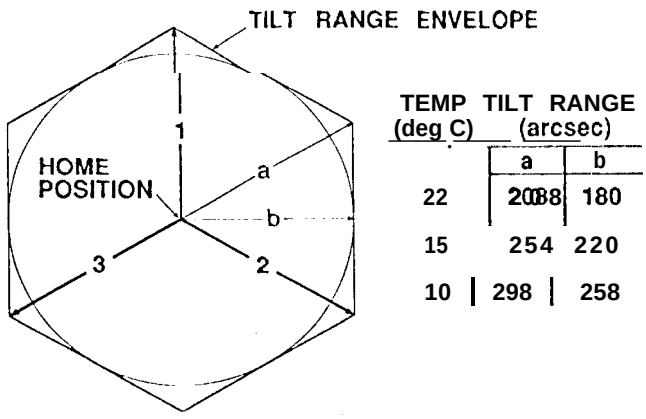

Fig. 9. Envelope of AFM tilt range showing actuator tilt basis vectors.

within the "shadow" of the pickoff mirror. The pickoff mirror is bonded to a bezel that is cinematically mounted to a two-axis flex-pivot gimbal. The bezel is articulated in two orthogonal axes (pitch and roll). Each axis is controlled by a lever that is connected via a leadscrew to a 28-volt, 4-phase stepper motor. The two stepper motors are only actuated when an adjustment of the POMM is required; they are powered off during normal camera operation. The device is designed with non-binding stops to prevent jamming. There are no sensors to determine position—a history file is maintained to track the position of each axis, and focal plane images are used to determine alignment.

3.3 Articulating Fold Mirror design

The Articulating Fold Mirror (AFM) provides tip and tilt control of the fold mirror. Three arc located in the fold mirror bulkhead at the front of the optical bench (see Fig. 1). The decision to include the AFMs was made late in the development of WF PC-2, and hence the design was driven by the need to package the device into a very compact space, such that they could replace the existing fixed fold mirrors without altering the optical design or the location of other existing components. The maximum front-to-back dimension was required to be less than 0.9 inches. This precluded the usc of conventional actuators such as stepper motors.

The AFM is derived from deformable mirror and active structure technology.[5] Each device utilizes six electrostrictive ceramic linear actuator segments, arranged in three pairs of two segments, as shown in Fig. 7. The linear expansion of each actuator is converted into a tilt of the mirror via a kinematic flexure mechanism. Each segment is independently addressable by the control electronics. Voltage is controllable to 8-bit resolution. Figure 8 plots the strain induced in an actuator as a function of applied voltage at several different temperatures. It is evident that the strain is very temperature dependent, and also exhibits hysteresis below room temperature. Interestingly, however, the material possesses a fiducial zero strain state; meaning that if the voltage is returned to zero, the strain returns to zero with no measurable offset. This is entirely unlike piezoelectrics, where remnant offsets arc typically as high as ten percent. This feature permits the AFM to be operated very precisely and repeatably, provided that the voltage is increased monotonically from zero to the desired value. The maximum voltage applied to the fright actuator segments is 88 volts.

Due to the 120-degree symmetry of the AFM mechanism, the envelope of achievable tilt angles is hexagonal, as shown in Fig. 9. Any point in the hexagon can be reached by commanding two of the three actuators, the third being left at zero volts. The vertex radius *a* corresponds to the tilt angle achieved by commanding onc or two of the actuators to full stroke (88 volts). The AFM mechanism produces a mirror tilt of approximately 206 arc scc for an actuator stroke of 4 μm (300 microstrain). The circular radius *b* corresponds to the maximum tilt range that can be achieved in all directions. Figure 9 lists values for *a* and *b* corresponding to three operating temperatures.

3.4 Flowdown requirements

Alignment stability depend.. on temperature stability in the case of the POMM, and on temperature and actuator drive voltage stability in the case of the AFM. Table 2 summarizes these flowdown requirements for both systems Alignment also depends on there not being any mechanical jitter. There are no separate flowdown requirements on jitter, because no sources of jitter could be identified within WFPC-2. Jitter in the HST was dccmcd not to be a problem based on WF/PC on-orbit experience and arguments of frequency separation between disturbances and mechanism/structure vibration modes.

The tight temperature stability requirements for the AFMs are due to the temperature sensitivity of the actuator material when it is electrically energized. In order to meet these requirements, an active temperature control system is implemented for the optical bench using replacement heaters and thermistors in onc of the electronics bays, While this is also implemented on WF/PC, the temperature range limits arc tightened on WFPC-2. The as-built performance of the AFM drive electronics is much better than the specification; for example, short term stability of the voltage was measured to be better than ±0.001 volt.

Table 2. Flowdown requirements on temperature and voltage stability

	POMM	AFM
temperature range:		
operate within spec.	-10"C – +25°C	+10°C - +14°C
survival	-30" C -- +25°C	-15°C - +20°C
temperature stability:		
short term (3oOO scc)	±1°C	±0.07° C
iong term	n/a	±1°C
voltage stability:		
short term (3000 scc)	n/a	***0.035** volt
long term	n/a	±0.25 volt

4. CALIBRATION AND DEVELOPMENT OF ANALYTICAL MODELS

4.1 Assembly level calibration of AFMs

Each AFM was calibrated as an assembly using an autocollimator with a resolution of 0.5 arc sec. Each of the six actuator segments was commanded to 90 volts in increments of 15 volts, and the corresponding mirror tilts recorded. The flight AFMs were calibrated at room temperature, while a flight spare AFM was calibrated both at room temperature and at the operational temperatures of 10° C and 15° C in a thermal vacuum chamber. The flight spare served as a transfer standard for extrapolating the flight unit data down to operational temperature. These calibration data formed the basis for the analytical model and software tool described in the following section.

Room temperature calibrations were repeated before and after major assembly level operations such as in-process vacuum bakeouts, certification bakeouts, mirror coating, etc. The AFMs were found to be extremely repeatable.

4.2 Analytical model for AFM motions

Laboratory calibrations of the AFMs provided tilt information at a small number of discrete voltages and temperatures. These data were used to constrain polynomial expressions for AFM dependence on both input voltage and operating temperature. The deflection versus voltage was modeled as the product of a functional shape, common to all actuators, and scale factor specific to each actuator segment. Experimentation with shape functions of the form

$$tilt = scale \times (b_2 v^2 + b_4 v^4 + b_6 v^6 + \ldots)$$

demonstrated that both second and fourth order terms in v were required for an acceptable fit, while sixth and higher term.. were not required or justified within errors of the laboratory measurements. After determining the two b_2 and b_4 coefficients which best fit the entire set of room-temperature laboratory AFM data, individual scale factors were determined for each actuator segment. In turn, the temperature dependences in the b_n coefficients were inferred

from measurements of the flight spare AFM, and modeled as $b_n = c_1 + c_2 t + c_3 t^2$. We compute the magnitude of AFM tilt for individual segments i as follows:

$$b_2 = (4307.0 - 185.7t + 2.98t^2) \times 10^{-7},$$

$$b_4 = (-2492.0 - 161.0t + 3.32t^2) \times 10^{-11},$$

$$tilt_i = scale_i \times (b_2 v_i^2 + b_4 v_i^4),$$

with $tilt_i$ in arc-seconds, t in degrees C, and $scale_i$ assigned specific values within the range 103--118 for the flight AFM segments. Finally, the magnitude and direction of tilt contributed by each actuator pair is projected onto appropriate orthogonal coordinates fixed in the optical assembly, so that the tilt vectors for all segments in a given AFM assembly can be added to give the resultant mirror tilt.

4.3 Algorithms for AFM commanding

The commanding algorithm must provide a transformation from voltage to mirror tilt which is smooth, with well-determined slope, to facilitate fine adjustments. The AFM model in the previous section is well suited to this requirement. We also require that the algorithm predict voltage settings which minimize temperature sensitivity. Minimum sensitivity to temperature for any required mirror tilt is obtained with approximately equal strain in both segments of a given pair, and with at least one actuator pair set to zero volts. 'l'he algorithm also carries out the conversion between AFM voltage source electronics command words (DN) and voltage applied to each segment, which laboratory measurements have shown to be an accurately linear transformation. For convenience, both segments of each pair are normally commanded to the same DN value. Finally, as a practical matter the transform should be invertable: DN ↔ voltage ↔ tilt. In order to minimize any AFM hysteresis effects, commands to the WFPC-2 AFMs normally include first a command to O DN on all actuator segments, followed by the command of one *or* two actuator pairs to the appropriate DNs.

Within the WFPC-2 optical system, coma induced by lateral misalignment of the pupil image projected on the corrective optics is linearly related to AFM tilts. The AFM alignment procedure involves first the analysis of star images to determine the magnitude and orientation of residual coma. The linear relationship between the induced coma and AFM tilt vectors then provides the guidance for AFM commanding.

4.4" Algorithm for POMM commanding

Commands to step the POMM change the pickoff mirror tilt along (approxirnately) orthogonal axes, with reference to absolute mirror position provided by a separate history of POMM commanding, As for the AFMs, the POMM predicted motions are projected onto an appropriate orthogonal coordinate system so that the effects of AFM and POMM tilts can be combined by vector addition.

5. SYSTEM LEVEL PERFORMANCE

5.1 System level alignment

The WFPC-2 optical system was aligned and verified with reference to a nurnbcr of optical test fixtures which simulated the aberrated HST wavefront. A critical step in the alignment of the WFPC-2 optical bench was the mounting of the four Cassegrain relay assemblies with the AFMs at their zero-voltage 'home' positions, a step which finalized six degrees of freedom in relay orientation including the lateral pupil alignment. Following this step, alignment was verified both by double-pass interferometry and by visual inspection of pinhole images with a microscope. In a final step, remaining coma was minimized by actuating first the POMM, to align the WFPC-2 optical axis with the simulator axis, then by applying small voltages to the AFMs to optimize relative pupil alignments among the four relay assemblies in the optical bench. These AFM voltages arc listed in Table 3. The mounting of CCD sensors, installation of the optical bench onto the instrument housing and flight latches, and addition of the remaining electrical and mechanical components completed the WFPC-2 integration.

5.2 Testing of the AFM and POMM stability

Knowledge of optical alignment stability is central to the development of strategies for efficient operation of WFPC-2 in the HST working environment. While the stability of the basic WF/PC optical system is well understood

from HST experience over the past three years, the mirror mechanisms are new and system performance needs to be verified with reference to the requirements in Tables 1 and 2. However, comprehensive tests of the end-to-end WFPC-2 alignment stability are difficult to implement, requiring both a level of thermal control and measurement sensitivity to mirror motions that are impractical in a vacuum test environment. Our tests were necessarily restricted to verification of the performance of subsystem over limited ranges in temperature.

A good monitor of the AFM stability is provided by illuminated points along the ridges of the four-faceted pyramid mirror (see Figure 2), known as 'K-spots.' These are lo-micron diameter pinholes, laser-drilled in the mirror coating and illuminated on command from behind by a number of small incandescent lamps set into a cavity on the backside of the pyramid mirror substrate, These points are imaged by the CCDs, and despite the spherical aberration induced by the corrective optics, a sharp central core in each K-spot image can be centroided to within about 0.1 pixel. Shifts in K-spot positions may arise from movement of any of the intervening optics, including the fold mirrors, Cassegrain relays, and CCD mountings. For example, Figure 10 illustrates the shifts in K-spot position due to commanded AFM tilts. The correspondence between K-spot shift and fold mirror tilt is about 16.4 arc-seconds per pixel for the WFC fold mirrors and 7.5 arc-seconds per pixel in the PC. Centroiding K-spots to within about 0.1 pixels gives a sensitivity of about 1 arc-second in the AFM mirror tilts.

Unfortunately, there was no comparably accurate measure of POMM stability during system level tests. The pickoff mirror position must be measured with reference to images projected by the optical 'Stimulus,' which provided the simulated HST beam used for both final optical alignment and the system-level verifications in the thermal vacuum test. The Stimulus is a large structure which exhibited RMS image motions as large as 0.6 PC pixels on time scales from seconds to hours, in response to both mechanical vibrations and thermal drifts in the test chamber. (As a consequence, all testing which required sharp images was carried out with flashlamps to 'freeze' the Stimulus motions.) Within the limitations imposed by Stimulus motion, the POMM showed no evidence of drift during the tests.

Table 3. Voltage settings for AFMs

channel	inital actuator voltages			current actuator voltages			magnitude of pupil shear	magnitude of coma*
	1AB	2AB	3AB	1AB	2AB	3AB	(% diameter)	(RMS waves)
PC1	17	0	20	23.3	0	0	0.68	0.059
WF3	**0**	**21**	**32**	7.4	0	29.2	1.03	**0.090**
WF4	**4**	**0**	**6**	**8.3**	**0**	**7.4**	**0.08**	**0.007**

• 1% *pupil shear* = 0.087 *RMS waves coma at S33 nm*[6]

5.3 Optical performance in system level tests

The K-spot positions were monitored before and after dynamics tests and throughout the systcm-level thermal vacuum test, providing our most sensitive indicator of the passive stability of the AFMs. The comparisons of K-spot positions before and after dynamics tests provided strong evidence of a robust optical alignment, since the WFCS showed shifts of approximately 0.1-0.2 pixels, while the PC K-spots shifted about 1.7 pixels. If these observed shifts were due entirely to fold mirrors, the stability against vibration would be consistent with the ground-to-orbit requirement in Table 1. It appears likely that the larger shift seen in the PC optics is duc to vibrational seating of the Cassegrain relay mounting, which is larger than the WFC relay assembly, and that the fold mirror shifts arc small in all four channels.

A 32-day system-level thermal vacuum test of WFPC-2 provided an accurate simulation of the thermal environment predicted for the HST, representing the range of thermal profiles experienced on orbit. The test provided the opportunity to validate and refine the AFM and POMM commanding algorithms and database, and to verify the functionality of the mechanisms. During the test. the POMM experienced a nearly constant temperature, while the AFMs were cycled through temperatures in the range 1O-14"C consistent with the limits to be maintained by an on-board application processor.

The overall optical alignment was periodically checked throughout the system level testing by analysis of out-of-focus images of a pinhole target, such as those in Figure 11. Out-of-focus images arc used because the PSF structure

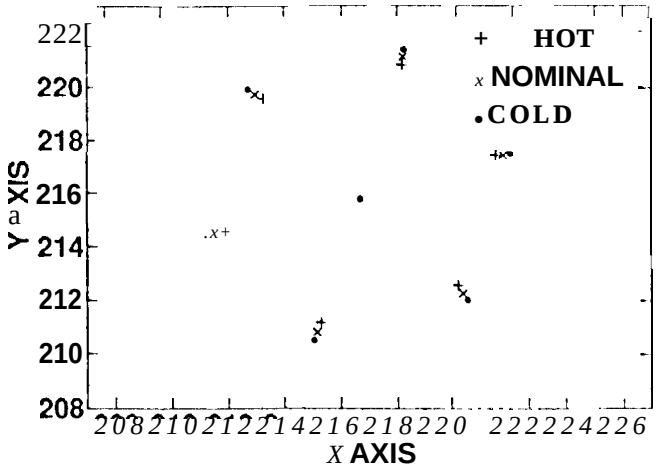

Fig. 10. Hexagonal tilt envelope of AFM at 42 volts for three temperatures based on the measurement of K-spot motions.

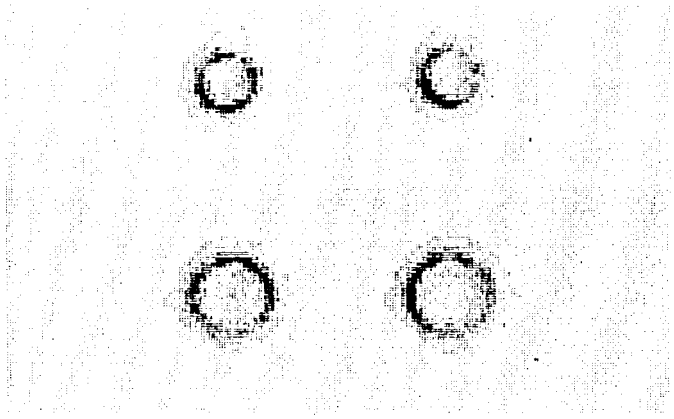

Fig. 11. Pinhole images on either side of best focus. Asymmetic brightness of the images is used to determine pupil shear.

in a focused image is inadequately sampled by the WFPC-2 (the first Airy ring has a diameter of 1.6 and 3.8 pixels in the WFC and PC channels respective] y), Out of focus, the wavefront information is distributed over a much larger number of pixels with a more uniform distribution of intensities. Such images can be analysed simultaneously for focus, coma, astigmatism, residual spherical aberration, and other wavefront aberrations; and peculiarities in the pupil illumination pattern can be isolated and distinguished from wavefront errors. This is indicated in Figure 11, where the asymmetric brightness distributions apparent in the images arise mostly from a combination of coma and non-uniform pupil illumination. Pupil illumination patterns invert upon passing through best focus, while the contributions from coma do not invert, as can be seen in the images.

Focus and coma characteristics were extensively explored and analysed during the trot. Due to the evident stability of the optical subsystem.., it was possible to regard the WFPC-2 wavefront error as the RSS summation of three components: focus, corns, and the additional terms 'built in' by design, figure of the optical components, and subsystem alignment. The RMS wavefront errors in the four channels, as determined in the thermal vacuum tests, are summarized in Table 4. Focus is explicitly separated from other wavefront errors in the table, while coma makes only a small contribution to the total when the optical system is otherwise well-aligned, as it was for the system level test.

Table 4. System level optical alignment[7]

	RMS wavefront error at 633 nm*			
	PC1	WF2	WF3	WF4
Without focus	**0.034**	**0.034**	**0.021**	**0.024**
with focus†	0.047	0.034	0.059	0.027

* *these data are preliminary*
† *includes effect of differential focus error*

Figure 10 illustrates two important characteristics observed during the thermal vacuum tests. First, the K-spot positions at a fixed voltage level (DN = 7B hex) show the temperature dependence of AFM stroke in each direction, as the AFM bulkhead temperature was stepped from 10 to 14° C during tests, Second, there is a small global shift between the the three complete patterns, which has been traced to a lateral shift in the CCI) position which is correlated with the temperature profile external to the WFPC-2 ('cold,' 'nominal,' and 'hot' orbital profiles). No anomalies have been observed in the AFM characteristics,

Table 3 lists the initial AFM settings determined during final optical alignment prior to installation of CCD sensors in December 1992. These were revised prior to system level dynamics tests in March 1993, and the revised

settings were used throughout the WFPC-2 thermal vacuum test. The current voltages, also listed in Table 3, are recommended for the initial AFM settings on-orbit. Final settings will be determined on the basis of the analysis of star images on-orbit. The magnitudes of pupil shear and coma listed in Table 3 correspond to the amount of alignment correction currently attributable to the AFMs.

In conclusion, we find that the active mirrors for WFPC-2 are performing nominally and provide the functionality needed to guarantee accurate correction of the HST aberrated wavefront. Since alignment of the optical system appears robust and requires only small AFM corrections at this time prior to launch, wc expect that the AFMs will be operated on-orbit with a fraction of the available stroke and therefore with a temperature sensitivity (which is proportional to stroke) well within the expected capabilities for temperature control.

6. ACKNOWLEDGEMENTS

Wc wish to acknowledge the contribution of the following individuals. Dwight Moody developed the algorithms and software for commanding the AFMs. Don Noon served as cognizant engineer for the Pickoff Mirror Mechanism development. Tom Radey served as cognizant engineer for the AFM electronics. Jim McGuire and Bob Korechoff performed the tolerancing and initial optical alignment of the WFPC-2 instrument. Robin Evans prepared the data for Figures 10 and 11.

Chris Burrows of the Space Telescope Science Institute performed the wavefront analysis in support of active optical alignment and system level performance measurements.

The Articulating Fold Mirrors were developed in partnership with Litton/Itek Optical Systems of Lexington, MA. Mark Ealey served as technical manager at Itek.

Finally, we wish to express their appreciation to the JPL WFPC-2 Project and to the Goddard Spaceflight Center for their support. The work described in this paper was carried out by the Jet Propulsion Laboratory, California Institute of Technology, under contract to NASA.

7. REFERENCES

1. J. T. Trauger and WFPC-2 Science Team, "Science with the Second Wide Field and Planetary Camera", in *Science* with *the Hubble* Space Telescope, ESO Proceedings 44, Sardinia, 1992.

2. A. H. Vaughan, "Diagnosing the optical state of the Hubble Space Telescope," *Jour. of the British Interplanetary Society*, Vol. 44, pp. 487-494, 1991.

3. D. H. Rodgers and A. H. Vaughan, "Wide-Field/Planetary Camera 11 for the Hubble Space Telescope service mission," Active and Adaptive *Optical Components and* Systems *II*, SPIE Vol. 1920, Albuquerque, 1993.

4. A. 13. Meinel and M. P. Meinel, "Two-stage optics: high acuity performance from low-acuity optical system..," **Optical** Engineering, Vol. 31, No. 11, pp. 2271--2281, 1992.

5. J. L. Fanson and M. A. Ealey, "Articulating Fold Mirror for the Wide-Field/Planetary Camera II," Active *and Adaptive* Optical *Components and Systems II*, SPIE Vol. 1920, Albuquerque, 1993.

6. J. P. McGuire and R. P. Korechoff, "Tolerancing of Wide-Field/Planetary Camera- I I," Quality *and* Reliability *for* Optical *Systems*, SPIE Vol. 1993, San Diego, 1993.

7. J. P. McGuire and R. P. Korechoff, "Optical alignment and ambient test of Wide-Field/Planetary Carrier-a -II," Optical Alignment, SPIE Vol. 1996, San Diego, 1993.